Improving Measurement Accuracy of Position Sensitive Detector (PSD) for a New Scanning PSD Microscopy System

Mehdi Rahimi[*], Yudong Luo[*], Frederick C. Harris, Jr[†], Sergiu M. Dascalu[†], and Yantao Shen[*]

Abstract—Measurement accuracy of Position Sensitive Detector (PSD) can be greatly affected by inaccuracies in interface circuits, system connections, outside environmental changes and the semi-conductive properties of the sensor. The presence of these factors causes noises and distortions that heavily degrade the performance of the PSD and any system built on it. This work addresses improving measurement accuracy of the PSD by using various correcting methods and filters to eliminate signal noises throughout the system and also develops a distortion rectifying methodology to rectify pincushion-type radial distortion associated with the PSD devices, which would enhance measurement accuracy in a larger active area of the PSD. Experimental validation demonstrates the effectiveness of these accuracy improvement methods. The improved PSD system can be further used for a proposed scanning PSD microscopy system. The system is capable of scanning an object in scale of a few micrometers for rapidly measuring the dimensions of the object based on the vanishing effect and the multi-channel photo-current feedback mechanism. Preliminary results show the measurement performance of the proposed microscopy.

I. INTRODUCTION

A Position Sensitive Detector/Device (PSD) is a sensor capable of tracking the location of a laser beam on its surface. A PSD consists of a uniform resistive layer formed on one or both surfaces of a high-resistivity semiconductor substrate and a pair of electrodes formed on both ends of the resistive layer for extracting position signals. The active area, which is also a resistive layer, has a P-N junction that generates photocurrent by means of the photovoltaic effect. PSDs can track very small positional changes of laser spot over the active area and directly output the position data with high resolution, high-speed response and high reliability [1]. There are two major types of PSDs available: Lateral PSDs and Segmented PSDs. In this work we focus on using a two-dimensional Lateral PSD. Lateral effect PSDs are continuous single element planar diffused photodiodes with no gaps or dead areas [2]. The factors that degrade the measurement accuracy of all types of PSDs generally include: (1) the aberration of the optical system, (2) the size of the light spot, (3) the position detection error of a PSD device and its

resolution, (4) the dark current and environment stray light, (5) the accuracy and noise level of the PSD detection circuit, (6) the temperature drift of the electronic circuit and optical system, (7) the tilting of the surface being measured, (8) the unevenness of the surface being measured, (9) the X-Y mismatch of the electrodes, (10) the difference of reflective characteristics of the surface being measured and (11) the distortions caused by the integration process of the PSD chip and its interface circuit. These factors strongly affect the position resolution and accuracy of a PSD system and are usually hard to be fully removed during the implementation of the PSD systems [1][3].

To improve the measurement accuracy of a lateral-effect PSD system, in this work, different noises are identified, analyzed, and eliminated by the signal averaging method. In addition, effects of X-Y mismatch and rotations are corrected. Finally, a distortion rectifying algorithm effectively solving pincushion-type radial distortions is developed. Both of the simulation and experimental results verify the effectiveness of the developed accuracy improvement methods. Such a PSD system with high reliability and accuracy can be further used for a proposed scanning PSD microscopy. The microscopy is based on the photo-current vanishing effect and the multi-channel photo-current feedback mechanism of the PSD. The vanishing effect is related to the four zero or low photo-current outputs when the laser beam is blocked by meeting the object on the PSD surface. Once the blocking positions of a scanning laser beam pattern are determined, the 2-D dimension of the micro object on the PSD surface can be accurately measured. Preliminary results on accurately and rapidly measuring both opaque and transparent objects demonstrate the performance of the proposed scanning PSD microscopy system.

The paper is structured as follows: In section II, the lateral effect PSD and the sensing system are introduced and some of its main properties are discussed. Section III is structured into four parts that describe our methods used to improve the accuracy of PSD, including a discussion about noises effecting the system and the used filtering method, the X-Y mismatch and rotation correction, the pincushion–type

---

[*] Mehdi Rahimi, Yudong Luo, and Yantao Shen are with the Department of Electrical and Biomedical Engineering, University of Nevada, Reno, NV 89557 USA (e-mail addresses: mrahimi@unr.edu; luoyudong1989@hotmail.com; ytshen@unr.edu).

[†] F. C. Harris, Jr, and S. M. Dascalu are with the Department of Computer Science and Engineering, University of Nevada, Reno, NV 89557 USA.

distortion and the proposed rectifying method, and mapping results after improvement. A new scanning PSD microscopy is discussed in detail in Section IV. The vanishing effect and the multi-channel photo-current feedback mechanism are described and preliminary experiments and results demonstrate the performance of the proposed microscopy. Section V concludes the work.

II. THE LATERAL EFFECT PSD AND SYSTEM

To implement our improvement methods, we have chosen a Duo-lateral effect PSD (OSI Optoelectronics DL-4S) for building up the testbed and modeling. The lateral effect PSD shown in Fig. 1-(a) is a 2-D sensor with $4mm \times 4mm$ active area. In a lateral effect PSD, the relative two-dimensional position of light beams such as a laser beam on the active surface of the chip can be expressed as:

$$X = \frac{I_{x1} - I_{x2}}{I_{x1} + I_{x2}} , \quad Y = \frac{I_{y1} - I_{y2}}{I_{y1} + I_{y2}} \quad (1)$$

where X represents the relative position of the laser spot on the X-axis and Y is the relative position on the Y-axis. Also $I_{x1}, I_{x2}, I_{y1}, I_{y2}$ are photo currents measured in the direction indicated by the index, which in the following experiments are called Channels A, B, C and D, respectively.

A very important property that has been used several times in the following experiments is that opposite channels have inverse correlation based on the structure of the PSD; this means when one of them increases, the other one decreases. This effect can be easily seen in Fig. 1-(b).
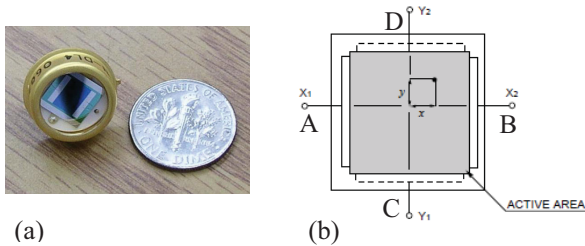

(a)   (b)

Fig. 1. (a) Photograph of lateral effect PSD chip; (b) Schematic illustration showing the two electrodes are mounted on opposite sides of the PSD to determine X-axis and Y-axis direction.

One major advantage of the lateral type PSD is the position linearity over relatively large areas of the active surface of the chip. This is important for our task since it allows us to keep errors at a low level during filtering, rectifying, and mapping processes. The signal conditioning circuit of the PSD can be employed and found in [4]. An overview of the whole PSD sensing system is illustrated in Fig. 2.

III. ACCURACY IMPROVEMENT METHODS AND EXPERIMENTAL VALIDATION

A. Noises and Filtering

There are different sources of noise for the whole system including the micro-manipulator motor that controls the laser, the ambient light on the PSD, the PSD board and its
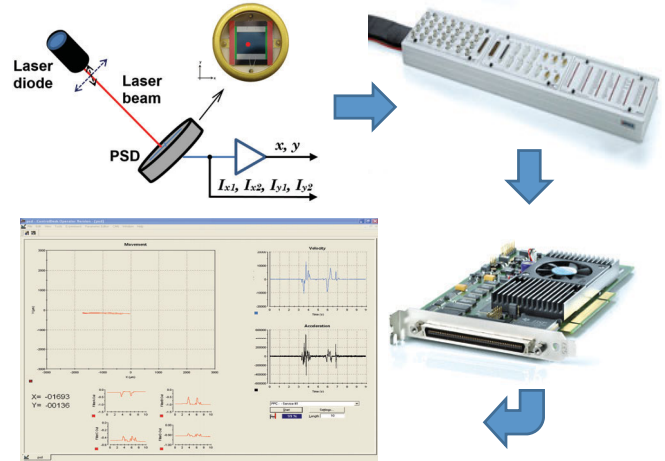

Fig. 2. The setup of the system is illustrated. PSD photo-current outputs are connected to the panel for dSPACE® DS1104 board which transmits the data to dSPACE® DS1104 R&D controller board. dSPACE® ControlDesk® designed program is used as PSD interface.

connections, the amplifiers, the probe, the dSPACE panel and control board that is used to get the data from the PSD board, and any movements in the area that may cause the PSD or the laser to shake. A set of tests were designed and ran to measure each of these noises and their impact on the system. The dSPACE noise is the most negligible noise as it produces a noise that results in less than 1μm movement in each direction which is shown in Fig. 3-(a). Another test measures the noise that the dSPACE and the PSD produce together but without any laser beam, meaning that it just shows the effect of ambient light and the noise of the PSD board. This is can be seen in Fig. 3-(b). We also noticed that the micro-manipulator motor that moves the laser has a considerable noise. This can be seen when comparing Fig. 3-(c) and Fig. 3-(d). And finally, the noise that the whole system produces when everything is on and the results can be seen in Fig. 3-(d). Notice that in all of these experiments, the motor is not receiving any command to move so the noise of the system is causing a vibration as high as almost 15μm in each direction. Fig. 3-(e) shows the noise after filtering and a zoom-in picture of the filtering versus noise is shown in Fig. 3-(f).

Fast Fourier Transform (FFT), is used as a powerful tool for analyzing and measuring noise signals as we can effectively measure the frequency content. Unfortunately, for this system is that, as it can be seen in Fig. 4, the noise does not occur in any special frequency. In other word, the system has a noise that is more similar to white noise. This means that the low-pass filters, band-pass filters, or similar approaches are not applicable for filtering out the noise of this system. In this experiment, the DC part of the signal is more important to us, we can use other methods to eliminate the noise. One can just use an AC to DC converter but that would remove useful information too. Finally we found out that signal averaging is a useful signal processing technique applied in the time domain, intended to increase the strength of a signal relative to noise that is obscuring it. By averaging a set of replicate measurements, the signal-to-noise ratio, S/N, will be
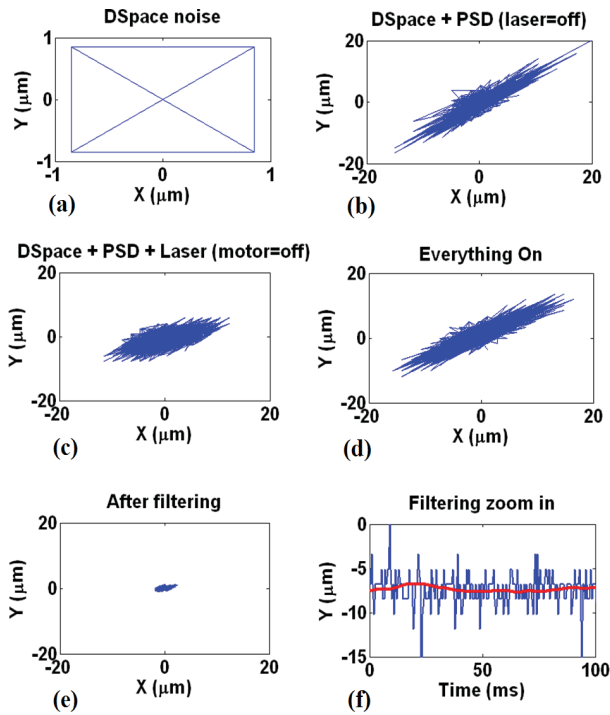
Fig. 3. (a) The noise that dSPACE produces results in less than 1μm movement in each direction; (b) The noise of the system when there isn't a laser beam on the PSD; (c) The noise of the whole system except the noise of the micro-manipulator motor; (d) The noise that the whole system produces when everything is on can be seen as an almost 15μm vibration in each direction; (e) The filtering has reduces the noise movement from 15μm to 1-2μm vibration in each direction; (f) A comparison of actual signal (blue) with the filtered signal (red graph in the middle) in an experiment. Note that all the figures have been centered for easier comparison.
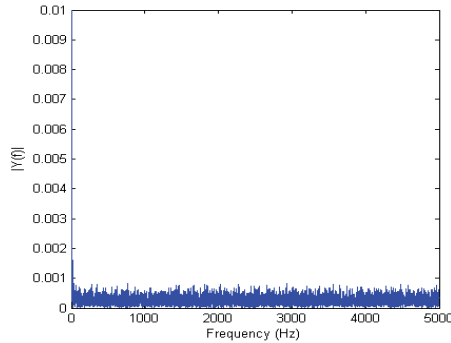

Fig. 4. FFT of the noise of the whole system doesn't show any particular frequency for the noise to filtering it out.

increased [5]. To prove this, suppose the noisy signal $v(k)$ is sampled every T seconds:

$$v(kT) = v_s(kT) + v_{noise}(kT) \quad (2)$$

If N partitions are composed, the averaged signal becomes

$$y(kT) = \sum_{i=1}^{N} v_s^i(kT) + \sum_{i=1}^{N} v_{noise}^i(kT), \quad (3)$$

$$\forall k=1,2,\ldots,M.$$

If the partitions are perfectly aligned and the signal is truly periodic, the desired signal adds up:

$$\sum_{i=1}^{N} v_s^i(kT) = N v_s(kT) \quad (4)$$

However, for Gaussian noise with zero mean and a standard deviation σ_n (which also equals its rms value), we obtain

$$\sum_{i=1}^{N} v_{noise}^i(kT) = \sqrt{N\sigma_n^2} = \sqrt{N}\sigma_n \quad (5)$$

Taking the ratio of (4) and (5), we can find the signal-to-noise ratio (SNR) after averaging N partitions:

$$SNR_N = \frac{N v_s(kT)}{\sqrt{N}\sigma_n} = \sqrt{N} \times SNR_1 \quad (6)$$

Thus, we get an $\sqrt{N}$ improvement in the SNR.

As the previous figures have shown, the mean of the noise is zero and we know that signal and noise are uncorrelated so signal averaging is the perfect solution in this case. The only disadvantage of this method is that it produces some amount of delay based on the period we use for averaging. The Simulink® modeling of this filter is shown in Fig. 5:
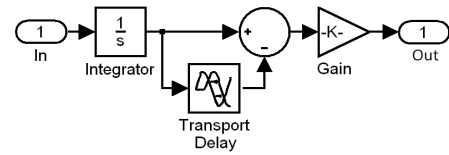

Fig. 5. Filter model in the Simulink

The gain block gives us 1/T where T is the time delay of transport delay block in seconds. The results in Fig. 3-(e) and Fig. 3-(f) show a significant improvement in noise reduction. The signal before filtering shows a vibration of about 15μm in each direction, but after the filtering the movement is limited to 1-2μm in each direction. This has been achieved without losing actual data. The filtered signal follows the actual signal perfectly and the maximum delay is less than 50 milliseconds.

B. X-Y Mismatch and Rotation Correction

It can be seen that in a PSD sensor, X and Y axes are not made perfectly perpendicular with each other and also the PSD is not parallel with the motor that moves the laser. The first problem results in X-Y mismatch and the second problem results in rotation of the whole coordinates. To match the two Cartesian coordinates that are on the PSD chip surface and on the position sensing software interface, a rotation matrix $\begin{bmatrix} \cos\theta & -\sin\theta \\ \sin\theta & \cos\theta \end{bmatrix}$ has been used to correct the mismatch between the two coordinates, where $\theta = 2.29$ is the calibrated mismatch angle between the coordinates. Similarly, to solve the problem of the X and Y axes not being perfectly perpendicular on the surface of the PSD, a skew matrix $\begin{bmatrix} 1 & \tan\varphi \\ 0 & 1 \end{bmatrix}$ was used, where $\varphi = -2.864$ was calculated.

C. Distortion Rectifying

The X and Y axes on the PSD have radial distortion. This means there is a deviation from rectilinear projection. The type

of radial distortion that the PSD has is called pincushion distortion. In pincushion distortion, the visible effect is that lines that do not go through the center of the image are bowed inwards, towards the center of the image. For correcting this distortion, Brown's distortion model [6] was employed. In this work, a version of the Brown's distortion presented by Villiers [7] with a slight modification was used:

$$x_u = (x_d - x_c)(1 + K_1 r^2 + K_2 r^4 + \cdots)$$

$$y_u = (y_d - y_c)(1 + K_1 r^2 + K_2 r^4 + \cdots)$$

$$r = \sqrt{(x_d - x_c)^2 + (y_d - y_c)^2}$$

$$(7)$$

Where (x_u, y_u) = undistorted point, (x_d, y_d) = distorted point, (x_c, y_c) = center of distortion and $K_n = n^{th}$ radial distortion coefficient. For this distortion, $K_1 = -0.62$ and $K_2 = 0.28$ were measured.

D. Mapping Validation

To evaluate the mapping performance after the coordinate rotation, correcting X-Y mismatches and rectifying the distortion, a focusable laser diode mounted on the 3-D precision moving stage was used to generate various laser traces onto the PSD. In Fig. 6-(a), a meander pattern was used to scan the whole surface of the PSD using the micro-manipulator as the reference. It became clear that the distortion is very noticeable. Using the above mentioned corrections the rectifying can be applied. The result of the rectified graph plotted in Fig. 6-(b) shows a very good mapping with the reference. It was measured that the mapping errors in X and Y are less than $20 \mu m$ which means less than 2%. The results clearly verify the good mapping performance by using the developed methods.

The meander pattern presents an acceptable distortion rectifying but it is actually a graph that just one dimensional parameter of X or Y changes each time. To scan the biggest area as possible of the PSD surface an Archimedean spiral was used. This spiral can be shown using the following formula:

$$x^2 + y^2 = a^2 (\tan^{-1} \frac{y}{x})^2 \qquad (8)$$

The result presented in Fig. 7 verifies the previous finding and both mapping errors in X and Y are within the range of $1 mm$ and less than 2%.

IV. THE SCANNING PSD MICROSCOPY

After achieving a PSD system with high reliability and accuracy, a new scanning PSD microscopy can be extended. The microscopy is based on the vanishing effect and multi-channel photo-current feedback mechanism of the accuracy improved PSD. In this section, we will detail the findings on this new microscopy.

A. Photo-current Output and Vanishing Effect

After extensive tests, it is clear that the effect of blocking the laser beam (called vanishing effect) can be determined by
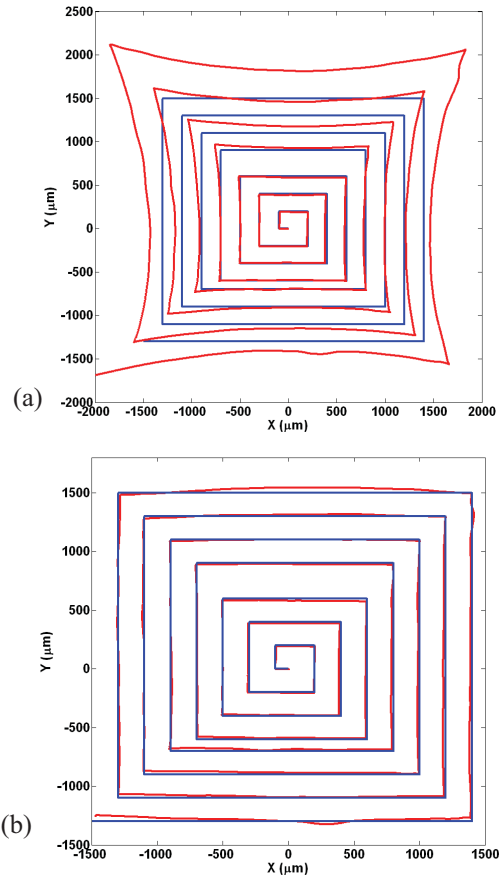

(a)

(b)

Fig. 6. (a) A meander pattern was used to determine the distortion (the red bigger graph). The blue graph is the reference; (b) signal after rectifying (red) versus the reference (blue).
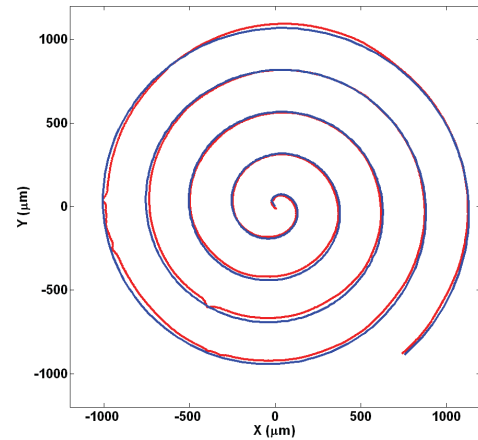

Fig. 7. Archimedean spiral was used to verify the results. The blue is the reference and the red is the rectified signal.

processing each of the 4 channels of the PSD individually. It was found that when there was a laser beam on the PSD, regardless of the position of the beam, each channel gives an output voltage of less than zero (because of the inverters in the PSD board). When the laser beam was blocked, they all quickly jump to zero. This effect generates distortion of scanning signals when there is an object on the PSD that blocks laser beam to photo detectors of the PSD. Fig. 8 demonstrate the distortion caused by laser blocking.

Based on this finding and the measurement accuracy improvement methods, a scanning PSD microscopy is proposed and preliminarily implemented. The mechanism of the microscopy is based on processing 4 photo currents from 4 input channels A, B, C, and D of the PSD and the developed accurate PSD mapping methodologies. More importantly, determining the occurrence of laser blocking on the PSD is the core of the microscopy, which can define the edge of the scanned object. Three methods were developed to determine the exact point that the blocking of the laser occurs.
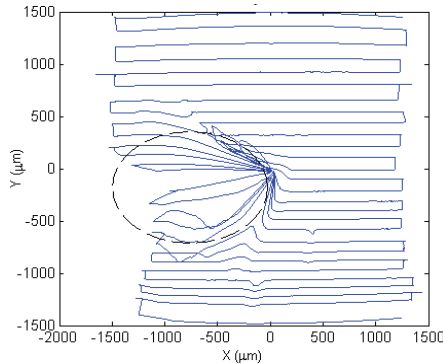

Fig. 8. The broken lines represent a small object that was placed on the PSD. The effect can be seen as blue lines.

B. Three Methods for Finding Laser Blocking Positions

1) Method 1

The first and the most accurate method is to monitor the smallest changes in two photo-current channels that are on opposite sides of the PSD. Using the property that was discussed in section II, it is known that these channels have inverse correlation. This means that when one of them increases, the other one decreases. On the other hand, from the previous section, it demonstrates that when an object blocks the laser beam, each channel immediately jumps to zero. These facts are presented in Fig. 9 and are used in the first method.
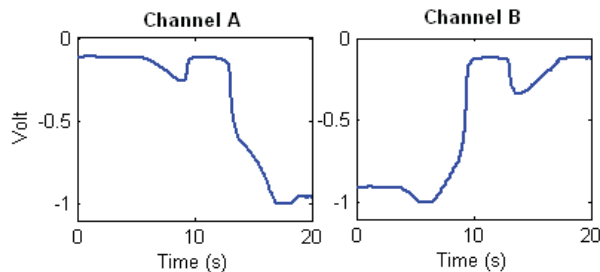

Fig. 9. The inverse correlation and jumping to zero of the output of two channels. The laser has started passing an object from second 10.

The program was developed and works as it starts monitoring each channel from the beginning and as it determines that the channels are no longer in an inverse correlation, it marks that point as the starting point of the blocking and with a similar approach, finds the stopping point. By calculating these two points, it can correct the object edge data in between and gives

us the size of the object. This determination can be found out easily with this formula:

$$((A(i) - A(i-1)) \times (B(i) - B(i-1))) < 0 \qquad (9)$$

Notice that it has been supposed that each photo-current changes smoothly but in practice it is not the case. As a result of this, the smallest noise can ruin this method and gives a false positive. To overcome this problem, the developed program first finds a peak in one of the channels and then goes back to find the starting point. Unfortunately, this approach makes the first method unusable in online plotting as it needs to go back and forth in time. That is the reason for implementing the second method.

2) Method 2

The second method determines the starting and stopping points by monitoring combined photo-currents $A + B$. The reason is, as it can be seen in Fig. 9, the inverse correlation between two channels can eliminate each other when added together in normal situations. When a block occurs, the addition of these channels can add up resulting in a bigger peak. This method is a bit less accurate as an exact specific point cannot be determined for every case but the advantage is that it can be used to correct the data online and generate the plots simultaneously. In this method, each time that $A + B$ becomes bigger than a specific set number (in this case, -0.9), a pass is marked and the starting and stopping points of the block can be extracted easily. Fig. 10 presents the effect of two passes on $A + B$.
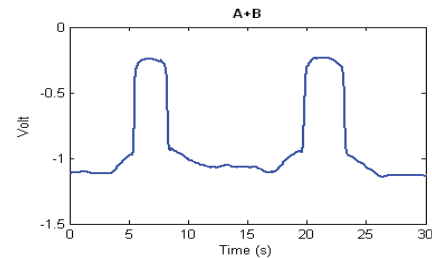

Fig. 10. Two passes leave a clear effect on A+B.

The second method covers most of the situations unless the object is transparent. In such a case, the laser beam would not be blocked completely and the result would be just the disturbance. In this case, monitoring A+B does not help as it does not clearly become bigger than a set point so the third method was designed.

3) Method 3

The third method uses the fact that when an object, even a transparent one, blocks the laser beam, there would be a disturbance in both channel photo-current A and B. To monitor this disturbance, the derivative of $A + B$ was used to find the point that $A + B$ starts changing rapidly. These sudden changes in $A + B$ determine a disturbance and consequently a pass. Fig. 11-(a) shows both channels A and B when the laser passes a transparent object. Fig. 11-(b) shows that the derivative of $A + B$ has some considerably big

peaks at the same time. This is because of the fact that it is showing the sudden changes in $A + B$ that is a result of the disturbance in each of the channels.

C. Measuring from Scanning

At this point we have all the solutions to measure the dimensions of an object. An experiment was designed to verify this ability. In this experiment, a SMD capacitor (1.57mm × 3.05mm × 1.57mm) was placed on the PSD surface. The laser performs a basic scanning and passes the object three times and the program uses the above mentioned methods to find each blocking occurrence location of the laser beam. The results and measurements for both channels A and B can be seen in Fig. 12.
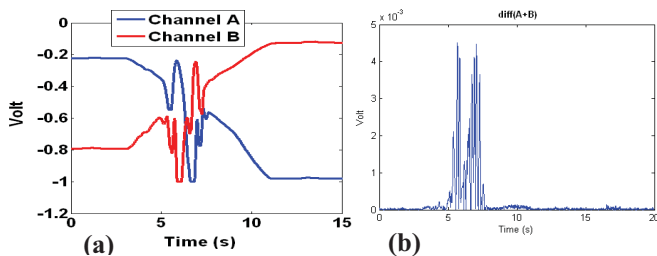

Fig. 11. (a) A pass of the laser over a transparent glass shows only a disturbance. (b) The derivative of A+B shows a disturbance from second 5 meaning a pass that lasts for about 2 seconds.
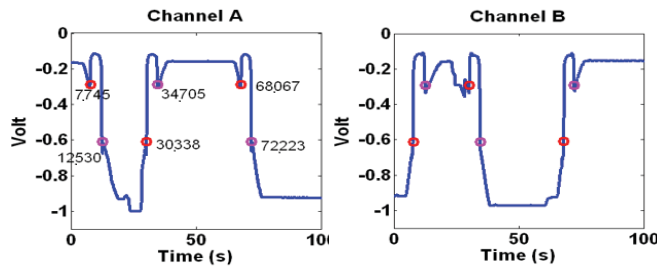

Fig. 12. The program finds the starting and stopping points for each passes of the laser beam over the object. Here there are three passes over the object.

Using the time of the starting point and stopping points of each pass, the program also shows the passes on an X-Y plot alongside the measurements of the object dimensions. This can be seen in Fig. 13-(a). Note that in this figure, dash lines were added later to represent the actual position of the object on the surface of the PSD. After extensive experiments with different objects it was determined that the measurements are promisingly accurate. Repeating the result gives a standard deviation of less than 6μm and the error in full range is less than 4%. It should be noted that the diameter of the laser beam we used is about 1mm itself. So by using a laser that is capable of producing a smaller beam and focusing it properly, the measurements could improve significantly. As it was discussed before in section IV-B, there is the third method for performing the same measurements for transparent objects. To verify that, another experiment was designed. In this experiment, a glass micropipette with an outer diameter of exactly 1mm was placed on the surface of the PSD and the laser beam scans the surface once from side to side. By monitoring the derivative of A+B the pass can be identified and the results can be seen in Fig. 13-(b).

Different experiments measured the size of the transparent glass micropipette were repeatable with an acceptable error with a standard deviation of less than 6μm. This validates that even transparent objects can be measured using the developed methods. The fact that the results are repeatable with very small error and standard deviation, proves that the system is promisingly working.
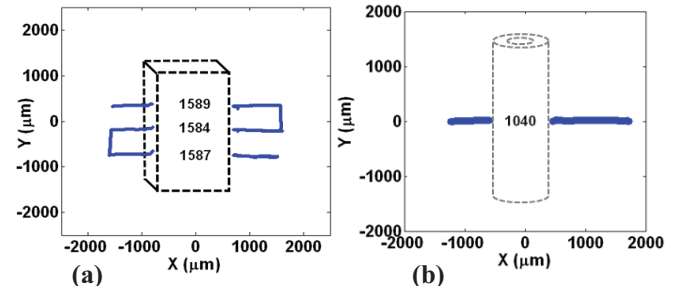

Fig. 13. (a)The program outputs an X-Y plot of the path that laser beam has travelled. (b) X-Y plot of the laser beam when passes over a transparent glass micropipette. Broken lines were added later to represent the object that was on the PSD surface.

V.   CONCLUSION

This work was started by studying a Position Sensitive Device (PSD) and its characteristics. We then examined and analyzed noises that the system is facing and used the signal averaging to greatly minimizing these noises. In addition, the X-Y mismatch and rotations were addressed, the PSD distortion was examined and the Brown's model was used to rectify the pincushion distortion. Extensive tests were run to verify and test the mapping of the data after all corrections. Later, a scanning PSD microscopy is proposed, its measurement mechanism is based on photo-current vanishing effect and feedback phenomena. Three different methods were designed and implemented to determine the occurrence of blocking laser (vanishing effect) on the PSD. Numerous tests and results prove that the PSD microscopy system is able to measure various objects, even a transparent object, with excellent accuracy and precision. The standard deviation of the measurements are less than 6μm and can be significantly improved in our future work.

REFERENCES

[1] Hamamatsu Selection Guide, PSD (Position Sensitive Detectors), *Solid State Division, Hamamatsu*, 2008.
[2] Technical Statement, PSD Characteristics, *OSI Optoelectronics*, webpage: www.osioptoelectronics.com.
[3] H. Spieler, "Chapter VI, Introduction to Radiation Detectors and Electronics," in *Position Sensitive Detectors*, 1998.
[4] OSI Optoelectronics, Duo-Lateral, Super Linear PSD's, page 48. webpage: www.osioptoelectronics.com.
[5] U. Hassan and M. S. Anwar, "Reducing Noise by Repetition: Introduction to Signal Averaging," *European Journal of Physics*, vol. 31, no. 3, p. 453, 2010.
[6] D. C. Brown, "Decentering Distortion of Lenses," *Photogrammetric Engineering*, vol. 32, p. 444–462, 1966.
[7] J. P. de Villiers, F. W. Leuschner, R. Geldenhuys, "Centi-pixel Accurate Real-time Inverse Distortion Correction," *Proceedings of International Symposium on Optomechatronic Technologies*, 726611, 2008.